

# PARAMAGNETIC DEFECTS IN SCHEELITE FROM GOLD QUARTZ VEIN DEPOSITS

DIRK HABERMANN<sup>(1)</sup>, ULF KEMPE<sup>(2)</sup>, FRANK WIRBELEIT<sup>(1)</sup>,  
MICHAEL PLÖTZE<sup>(3)</sup> AND JÜRGEN. R. NIKLAS<sup>(1)</sup>

<sup>(1)</sup> *Institute of Experimental Physics, University of Technology and Mining Freiberg (Germany)*

<sup>(2)</sup> *Institute of Mineralogy, University of Technology and Mining Freiberg (Germany)*

<sup>(3)</sup> *Institute of Geotechnics, ETH Zürich (Swiss)*

**KEY WORDS:** Scheelite, Au-deposit, Electron spin spectroscopy (ESR), paramagnetic defects

## INTRODUCTION

Two models of the genetic relationship between Au and W in mesothermal Au-quartz deposits are still in discussion. The first one is a coincidental model describing the overlapping of two different processes of formation (e.g. Luukkonen 1994) while the second one bases on the assumption of a close association of Au and W (e.g. Afanas'eva et al. 1995).

Investigations by Kempe & Oberthür (1997) on scheelite from Au-(W) and W-Sb mineralization revealed that grayish, brownish, and yellowish to orange coloration are common and possibly caused by radiation damage due to high uranium content with generation of color centers. These innocent radiation defects are probably localized on the [WO<sub>4</sub>] tetrahedron. These centers seem to have also a great influence the luminescence of scheelite additional to that of activator elements (e.g. some rare earth elements (REE)). It was found that MREE, HREE, and Sr enrichment together with low Mo contents are characteristic for scheelite from Au-(W) deposits. As mostly trivalent REE are incorporated in Ca-position charge compensation can be provided by electronic defects like defect electrons and defect ions located at the [WO<sub>4</sub>] tetrahedron, on Ca-positions, or on interstitial positions. However, the chemistry and atomic defect structure are possibly correlated with the conditions of ore formation.

Our work is focused on the investigation of the atomic defect structure of scheelites from Au-W deposits of Muruntau and Myutenbaj (Uzbekistan), Kasparske Hory (Czech Republic), Khovd gol (Mongolian Altai), Berezovskoe and Pelengichej (Urals), and Stori's (Zimbabwe). Sixteen samples of sufficient size, various coloration (white, grayish, brownish-yellow to orange and brown) and trace element chemistry (differing mostly in REE and U concentrations) were selected and analyzed by ICP-MS, optical spectroscopy, cathodoluminescence (CL) spectroscopy and Electron Spin Resonance spectroscopy (ESR) (X-Band). The results from the ESR analyses of paramagnetic defects are presented and discussed in this work.

## CONCLUSIONS

The ESR spectra of scheelites from Au-(W) deposits show three groups of signals at room temperature and at 70° K. Most of them - particularly the signals of the second group - were not detectable in scheelite from other types of W-bearing deposits (cf. Plötze et al. 1994) and up to now were not described in the literature.

- 1) The first group includes well-known signals from paramagnetic centers related to elements incorporated on Ca position in the scheelite structure. It was found that most samples are containing  $Mn^{2+}$ , yielding typical ESR spectra with thirty lines with the magnetic field  $B_0$  in parallel to the crystal axis  $c$  ( $g$ -factor at 1.9998; see Fig.1). Most samples also show lines related to  $Gd^{3+}$  with  $g_{II}=1.9915$ . These signals are commonly found also in scheelite from other types of W-bearing deposits.
- 2) A second group of signals in the ESR spectrum of Au-(W) deposits is indicated by sets of lines indicated formally by  $g$ -values between  $g \sim 6.3$ -28 and  $g \sim 1.3$ . These lines seem to be diagnostic for scheelite from Au-W deposits and they are described here for the first time. Fig. 2a/b shows such typical ESR spectra of a brownish-orange scheelite from Muruntau (W-Uzbekistan) with  $B_0$  parallel  $c$  (Fig. 2a) and perpendicular  $c$  (Fig. 2b). By different angular dependencies, line splitting, and by the equidistant lines of the second group, different kinds of defects can be distinguished. The set of lines marked with **-A-** were simulated using a multi spin simulation (Fig. 2a). It was found that five fine structure (fs) lines with the central transition at  $g=3.745$  can be attributed to a defect model with  $S = 5/2$ ,  $I = 1/2$ ,  $D = 4350$  MHz (large zero field splitting) for  $B_0$  parallel  $c$ . The strong asymmetry of the ESR signals indicates that fs lines **-A-** are partly overlapped by the signals of the set **-B-**. The latter can be simulated with  $g=3.680$ ,  $S = 5/2$ ,  $I = 1/2$ ,  $D = 4300$  MHz. This defect is considered as the same kind of ion (most probably  $Fe^{3+}$  -see below-) but in slightly different lattice position compared to **-A-**. For  $B_0$  perpendicular to  $c$  (Fig. 2b) some lines can be simulated by the parameters  $S = 5/2$ ,  $I = 1/2$ ,  $D = 500$  MHz and  $g$ -values at 3.6 (**-a-**) and 3.509 (**-b-**). These signals apparently belong to another defect. We suppose it as a  $Fe^{3+}$  likely defect not related to **-A-** and **-B-**. The latter can be on principle explained by the angular dependence (simulated) resulting from a  $S=5/2$  system with  $g$  is isotropic and strong influence of the fs-interaction, see (Fig. 3).  
A signal **-C-** ( $g^{\wedge}=2.9$  in Fig. 2b) increased in intensity when the crystal is rotated around an axis perpendicular  $c$ . The maximum intensity and line splitting was observed for  $B_0$  approximately 90° off  $c$ . These lines are partly overlapped by lines of **-a-** and **-b-**. So part of this signal based on the superposition of lines from **-a-** and **-b-**. Nevertheless these signals (**-C-**, **-a-**, **-b-**) are only present in scheelite from Au-(W) deposits and are therefore seems to be also indicative for scheelite from Au-W deposits.

- 3) A third group of signals has g values of about 2 at c parallel  $B_0$ . The g-values of around 2 are explained by electronic defects located at the  $WO_4$  and  $SiO_4^{3-}$  tetrahedrons. Detailed analyses of the spectral region at  $g=2$  indicates lines of the  $SiO_4^{3-}$  at  $g_z = 2.017$  and a signal at  $g_z = 2.003$  the origin of which is probably related to electron defects located at a distorted  $W(Fe)O_4$  tetrahedron.

In our samples these signals are observed in basically grayish, and brownish to red colored samples and seem also positively correlated with the content of uranium. The latter was earlier documented by Kempe and Oberthür (1997). All orange samples show the signal at  $g_z = 2.003$  additionally to the signals of sets -A-, -B-, -a-, -b- and -C-. It seems possible that the signal at  $g_z = 2.003$  is correlated with these defect species and the  $REE^{3+}$  content in scheelite.

Comparable spectra to set -A- and -B- are known from other minerals and attributed to  $Fe^{3+}$  ( $S = 5/2$ ,  $I = 1/2$ ) in tetrahedral lattice position (Petrov & Hafner 1988). Petrov et al. 1989 assigned the lines with g-values of 19.3, 4.8, 3.3, 2.3 and 1.3 to  $Fe^{3+}$  in tetrahedral position in albite. However, the  $WO_4$  tetrahedron of scheelite is slightly different in symmetry and atomic distance between the O-ligand and central metal ion compared to the feldspar structure. The  $Fe^{3+}$  ion is small, having an ionic radius of 0.65 Å, more similar to  $W^{6+}$  (0.62 Å) than to  $Ca^{2+}$  (1.0 Å). In principle, both lattice site positions and interstitial positions are possible. For the  $Ca^{2+}$  position, only one additional negative charge is required, but three negative charges are required for the W position. The charge compensation may be related to different kind of defects. For example, e<sup>-</sup>-vacancies located on oxygen ions, oxygen vacancies,  $Ca^{2+}$  vacancies and  $REE^{3+}$  ions on Ca sites are possible solutions to the problem. The latter is more likely, however, the  $REE^{3+}$  concentration seems to be positively correlated with the intensity of the EPR signal at  $g \sim 45-28$  and  $g \sim 3.7$  as revealed by ICP-MS and CL data.

Comprehensive, scheelite from Au-(W) deposits shows specific signals in the ESR spectrum contrary to scheelite from other mineralizations. Here, both the visible coloration and the paramagnetic defect properties are characteristic. It is possible to use scheelite as a pathfinder in Au exploration using ESR spectroscopy.

The coloration of these scheelites is mostly a mixture of different basic colors possibly related to different electron defects located at the tetrahedron. Significantly, purr gray colors are only documented in samples with high uranium, very low REE concentration and no or minor intense signals of the second group paramagnetic defects. Electronic defects at the  $WO_4$  tetrahedron are the most possible explanation. Basically red colors are related to  $SiO_4^{3-}$  defects. Orange to yellowish colors are characteristic for samples, where the EPR signals of the second group and the signal at  $g_z = 2.003$  are present and where REE are incorporated in scheelite structure in sufficient quantities.

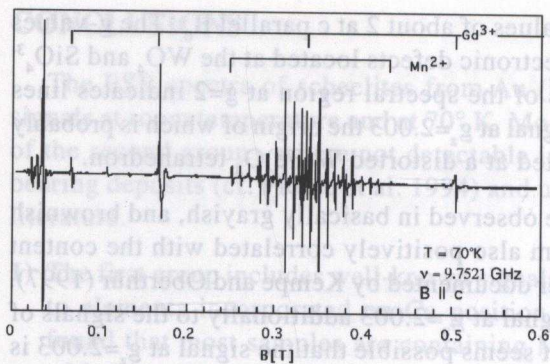


Fig. 1: First derivative ESR spectrum at  $T=70^\circ\text{K}$  and  $B_0 \parallel c$  of a scheelite single crystal from Stori's (Zimbabwe).

Fig.2a

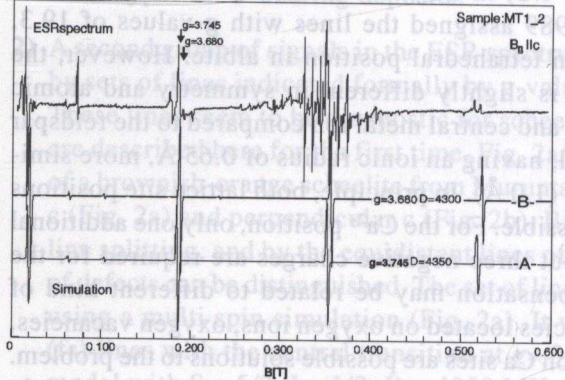


Fig. 2a/b: First derivative ESR spectra of a brownish-orange scheelite from Muruntuau (Uzbekistan). Spectrum at  $T=300^\circ\text{K}$  and  $B_0 \parallel c$  and  $B_0 \perp c$ .

a)  $B_0 \parallel c$ : The asymmetry of the ESR signals at  $g \sim 4.4-3.4$ ,  $3.745$ ,  $3.60$ ,  $\sim 2$  and  $\sim 1.3$  indicates the overlap of two sets of lines, most probably attributed to  $\text{Fe}^{3+}$  located at slightly different lattice positions.

Fig.2b

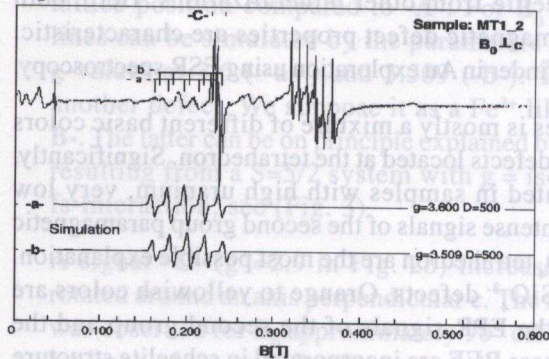


Fig. 2b: The signals with central transition  $g=3.509$  and  $3.6$  show also a strong asymmetry in the lineshape. These lines are possibly caused by  $\text{Fe}^{3+}$  in different lattice positions as attributed to -A- and -B- (see text and Fig.3).

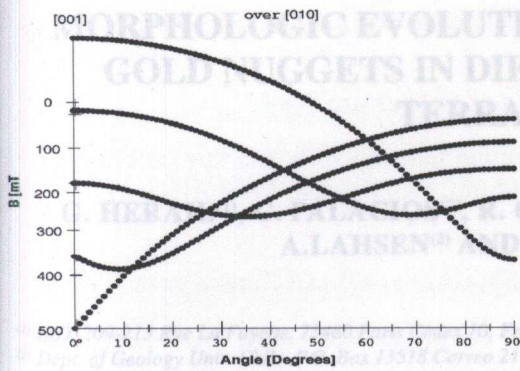


Fig. 3: Angular dependence (simulation) of the ESR spectrum of a  $S=5/2$  system.  $g$  is assumed to be isotropic  $D/g\mu_B \ll B_0$  ( $D/g\mu_B = 4300$  MHz).

KEY WORDS: Gold grains, morphologic evolution, different climates, exploration

## ACKNOWLEDGMENTS

The investigations were supported by a grant of the German Science Foundation (DFG Ni 161/5-1).

## REFERENCES

- Afanas'eva Z.B., Ivanova G.I. & Raimbault L. (1995). Scheelite as an indicator of formation-conditions of gold-sulfide mineralization: The Olimpiada Au-(Sb-W) contact metamorphic deposit, Russia. In J. Pasav., T. Kribek and P. Z'k (eds.), Mineral deposits: from their origin to their environmental impact. Rotterdam: Balkema. 835-838.
- Kempe U. & Oberthür T. (1997). Physical and geochemical characteristics of scheelite from gold deposits: A reconnaissance study. In H. Papunen (ed.), Mineral deposits: Research and Exploration where do they meet? Rotterdam: Balkema. 209-212.
- Luukkonen A. (1994). Main geological features, metallogeny and hydrothermal alteration phenomena of certain gold and gold-tin-tungsten prospects in Southern Finland. Bulletin of the Geological Survey of Finland. 377.
- Petrov I. & Hafner S.S. (1988). Location of trace  $Fe^{3+}$  ions in sanidine,  $KAlSi_3O_8$ . Am. Min. 73. 97-104.
- Petrov I., Yude F., Bershov L.V., Hafner S.S., & Kroll H. (1989). Order-disorder of  $Fe^{3+}$  ions over the tetrahedral position in albite. Am. Mineralogist. 74. 604-609.
- Plötze M., Kempe U. & Wolf D. (1994). EPR-Untersuchungen an natürlichen Scheelitkristallen bei tiefen Temperaturen. European Journal of Mineralogy. v6. n1. 214.

Blaze M., Kempe U. & Wolf D. (1994). EPR-Untersuchungen an natürlichen Schmelzkristallen bei tiefen Temperaturen. *European Journal of Mineralogy*, **6**, 211-214.

Blaze M., Kempe U. & Oberhür T. (1997). Physical and geochemical characteristics of schistite from gold deposits: A reconnaissance study. In H. Papunen (ed.), *Mineral deposits: Research and Exploration where do they meet?* Rotterdam: Balkema, 209-212.

Butkovich A. (1994). Main geological features, metallogeny and hydrothermal alteration phenomena of certain gold and gold-tungsten prospects in Southern Finland. *Bulletin of the Geological Survey of Finland*, **377**.

Stov I. & Hahnert S.S. (1988). Location of trace  $Fe^{2+}$  ions in sandine, KAISI<sub>2</sub>O<sub>6</sub>. *Am. Min.* **73**, 97-104.

Stov I., Barabov L.V., Hahnert S.S.; & Kroll H. (1989). Order-disorder of  $Fe^{2+}$  ions over the tetrahedral position in albite. *Am. Mineralogist*, **74**, 804-809.

Kannan S.V., Ivanova G.J. & Rajambal J. (1992). Schistite as an indicator of formation conditions of gold-sulfide mineralization: The Olympia Au-(Sb-W) contact metamorphic deposit, Russia. In J. Pasav., T. Kříbek and P. Žák (eds.), *Mineral deposits: from their origin to their environmental impact*. Rotterdam: Balkema, 835-838.

ACKNOWLEDGMENTS

The investigations were supported by a grant of the German Science Foundation (DFG Nr. 1615-1).

Fig. 2b: First derivative ESR spectra of schistite from the Uchekistun Spec (Kashmir), H.c. and B.L.c.

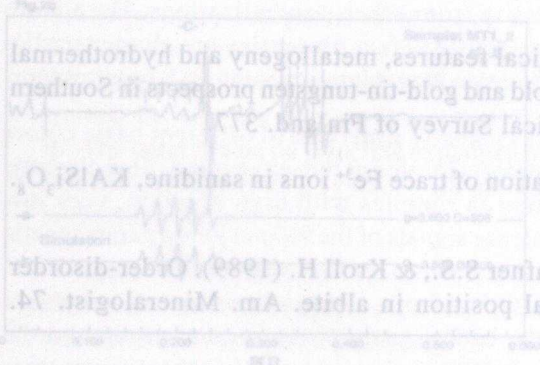


Fig. 2b: First derivative ESR spectra of schistite from the Uchekistun Spec (Kashmir), H.c. and B.L.c.

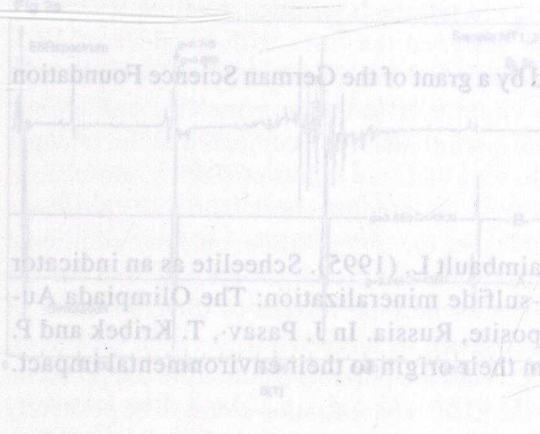


Fig. 2a: First derivative ESR spectra of schistite from the Uchekistun Spec (Kashmir), H.c. and B.L.c.

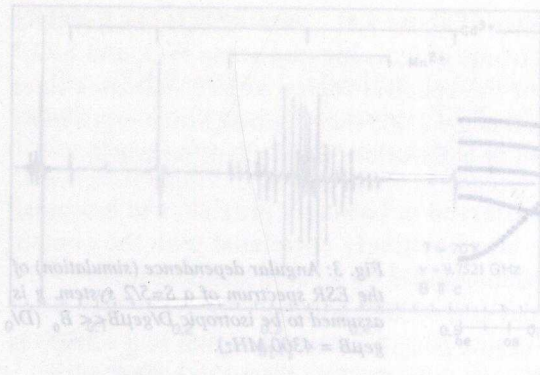


Fig. 1: Angular dependence (simulation) of the ESR spectrum of a 2x2x2 system. The curves are assigned to isotropic  $g$ -factor  $g_{iso} = 4.300$  MHz.

Fig. 1: First derivative ESR spectra of schistite from the Uchekistun Spec (Kashmir), H.c. and B.L.c.